Received: 22 May 2018 | Revised: 4 December 2018 | Accepted: 14 December 2018

DOI: 10.1111/ejn.14331

RESEARCH REPORT

WILEY EJN European Journal of Neuroscience FENS

Feeding cycle alters the biophysics and molecular expression of voltage-gated Na^+ currents in rat hippocampal CA1 neurones

André E. P. Bastos[1,2,3] | **Pedro F. Costa**[2] | **Suzy Varderidou-Minasian**[4] | **Maarten Altelaar**[4] | **Pedro A. Lima**[2,3]

[1]Department of Chemistry and Biochemistry, Centre of Chemistry and Biochemistry, Faculty of Sciences University of Lisbon, Lisbon, Portugal

[2]Department of Physiology, Nova Medical School/Faculdade de Ciências Médicas, Lisbon, Portugal

[3]Sea4Us, Biotechnology and Marine Resources, Lda., Sagres, Portugal

[4]Biomolecular Mass Spectrometry and Proteomics, Utrecht University, Utrecht, The Netherlands

Correspondence
Pedro A. Lima, Department of Physiology, Nova Medical School/Faculdade de Ciências Médicas, Lisbon, Portugal.
Email: pedro.lima@nms.unl.pt

Funding information
Sea4Us, Biotechnology and Marine Resources, Ltd.; Fundação para a Ciência e a Tecnologia, Grant/Award Number: SFRH/BD/88199/2012; Prime XS, Grant/Award Number: PRIME-XS-000226

Abstract

The function of hippocampus as a hub for energy balance is a subject of broad and current interest. This study aims at providing more evidence on this regard by addressing the effects of feeding cycle on the voltage-gated sodium (Na^+) currents of acutely isolated Wistar rat hippocampal CA1 neurones. Specifically, by applying patch clamp techniques (whole cell voltage clamp and single channel in inside-out patches) we assessed the influence of feeding and fasting conditions on the intrinsic biophysical properties of Na^+ currents. Additionally, mass spectrometry and western blotting experiments were used to address the effect of feeding cycle over the Na^+ channel population of the rat hippocampus. Na^+ currents were recorded in neurones obtained from fed and fasted animals (here termed "fed neurones" and "fasted neurones", respectively). Whole cell Na^+ currents of fed neurones, as compared to fasted neurones, showed increased mean maximum current density and a higher "window current" amplitude. We demonstrate that these results are supported by an increased single channel Na^+ conductance in fed neurones and, also, by a greater Nav1.2 channel density in plasma membrane-enriched fractions of fed samples (but not in whole hippocampus preparations). These results imply fast variations on the biophysics and molecular expression of Na^+ currents of rat hippocampal CA1 neurones, throughout the feeding cycle. Thus, one may expect a differentiated regulation of the intrinsic neuronal excitability, which may account for the role of the hippocampus as a processor of satiety information.

KEYWORDS

CA1 neurones, feeding cycle, ion channels, rat hippocampus, voltage-gated sodium currents

Abbreviations: a_f, amplitude coefficient of the fast component of inactivation; a_s, amplitude coefficient of the slow component of inactivation; E_{Na}+, Reversal potential of Na^+ ions (mV); h_∞, steady-state of inactivation curves; I_{Na}, Voltage-gated Na^+ currents; *I-V*, Current to voltage relationship; $Na_v1.2$, Voltage-gated sodium channel protein type II subunit alpha; V_h, Half-maximal activation (or inactivation) potential (mV); V_s, Slope factor (mV/*e*-fold); τ_h, Time-constant of inactivation (ms); τ_{hfast}, Time-constant of the fast component of inactivation; τ_{hslow}, time-constant of the slow component of inactivation.

Edited by Marco Capogna. Reviewed by Yunlei Yang and Emma Louth.

All peer review communications can be found with the online version of the article.

1 | INTRODUCTION

The involvement of the brain upon feeding and energy balance, by a concerted endeavour of different brain areas, has been documented (Davidson, Kanoski, Schier, Clegg, & Benoit, 2007; Tracy, Jarrard, & Davidson, 2001). The hippocampus, historically seen as a substrate for learning and memory processes, has also been implicated in such energy regulation: (a) hippocampus contains receptors for several hormonal signals of relevance to energy status, as leptin, ghrelin, and insulin (Beck & Pourié, 2013; Diano et al., 2006; Hsu, Suarez, & Kanoski, 2016; Hsu et al., 2015; Lathe, 2001); (b) it integrates a neuronal circuitry that involves several regions of the brain (e.g. hypothalamus) responsible for ingestive and appetitive behaviours (Sweeney & Yang, 2015, 2017); (c) it perceives interoceptive signals (energy state cues like hunger and satiety) to modulate the feeding behaviour (Davidson & Jarrard, 1993; Scoville & Milner, 1957); d) given its role in episodic-meal related memories, the hippocampus inhibit meal onset during the postprandial period (Benoit, Davis, & Davidson, 2010; Davidson, Kanoski, Walls, & Jarrard, 2005; Hannapel, Henderson, Nalloor, Vazdarjanova, & Parent, 2017; Henderson, Smith, & Parent, 2013; Kanoski & Grill, 2017; Parent, 2016a; Parent, Darling, & Henderson, 2014; Tracy et al., 2001).

The increasing compelling evidence that portraits the hippocampus as a hub for energy homeostasis has contributed to the development of studies designed to comprehend the effects of nutrition on cognition and, consequently, on appetite. Indeed, there is emerging research referring to the diet-mediated modulations of adult hippocampal neurogenesis (Stangl & Thuret, 2009), functioning (Cansev et al., 2015; Kanoski & Davidson, 2011; Yeomans, 2017), and structure (Jacka, Cherbuin, Anstey, Sachdev, & Butterworth, 2015) as possible mechanisms by which nutrition impacts on neuronal function.

Still, the effect of feeding cycle on neuronal activities is scarcely understood, especially in the hippocampus. There is a single work showing that the effect of insulin on the excitability of rat hippocampal CA1 neurones (Lima, Vicente, Alves, Dionísio, & Costa, 2008) is only detectable in fed animals, contrasting with the lack of response in fasted ones (Lima et al., 2012). This clearly suggests a marked impact of feeding cycle periods over the activity of central nervous system neurones, particularly in protein ion channels involved in excitability.

This finding has urged further investigation to evaluate the effect of feeding cycle upon the activity of other ion channels. Given the seminal role of the voltage-gated sodium (Na^+) currents/channels in the initiation and propagation of action potentials (hence, in the control of neuronal excitability levels), we aimed at assessing whether feeding cycle affects the biophysics and expression of voltage gated sodium (Na^+) currents (I_{Na}) of acutely isolated rat hippocampal CA1 neurones. The regulation of such currents by the feeding cycle may contribute to the alterations of neuronal behaviour.

Our results show that neurones from fed animals (here termed "fed neurones", as oppose to "fasted neurones" obtained from fasted animals) disclosed an increased whole-cell Na^+ current density and larger single-channel conductance. Fed neurones (in comparison to fasted neurones) also revealed a hyperpolarizing shift of the activation curves and a depolarizing shift of the steady-state inactivation curves, which resulted in a greater amplitude of the respective "window current". This is consistent with a greater steady-state channel availability (Huang, Priori, Napolitano, O'Leary, & Chahine, 2011; Ruben, Starkus, & Rayner, 1992; Vedantham & Cannon, 1998). Accordingly, we detected that the neuronal plasma membrane of fed animals presented a higher concentration of $Na_v1.2$, the major α-subunit of the rat brain (Gordon et al., 1987). In addition, still in fed neurones, we have obtained a depolarizing shift in the voltage dependence of the time-constant of the slow inactivating component (τ_{hslow}) of I_{Na}. By all accounts, these alterations in the biophysical and biochemical properties of I_{Na} suggest a higher level of excitability in rat hippocampal CA1 neurones upon feeding.

Through a combination of electrophysiological and molecular biology methods, we indicate I_{Na} as hallmarks in the impact of feeding cycle in acutely isolated rat hippocampal CA1 neurones. This provides new insights into a possible involvement of voltage gated Na^+ channels towards the regulation of energy balance by the hippocampus.

2 | MATERIALS AND METHODS

2.1 | Ethical approval

All the procedures involving animal subjects, namely neuron and brain preparations, were performed upon approval by the Ethical Committee of the Nova Medical School from NOVA University (14/2015/CEFCM), and according with the European and Portuguese guidelines for the protection of animals used for scientific purposes (European Union Directive 2010/63/EU, transposed to Portuguese Legislation by the Decrete DL 113/2013).

2.2 | Animal monitorization

Twenty-one- to 29-day-old female Wistar rats (P21-29), purchased from Charles River Laboratories, were used according to Afonso et al. (2012). Briefly, animals were maintained under a 12:12 hr light/dark cycle with free access to food and water. On the day before the experiment, animals were subjected to an overnight fasting period, in which the effect of

food deprivation is greatest (Palou, Remesar, Arola, Herrera, & Alemany, 1981), with the free access to water maintained. At the day of the experiment, animals were either fed during a period of 1 hr to ensure that they had eaten by the time the experiment started (here termed fed animals or "fed neurones") or not fed (here termed fasted animals or "fasted neurones").

Afterwards, the animals were killed by cervical dislocation and the brain was rapidly removed from the skull and placed in chilled artificial cerebrospinal fluid (ACSF) containing (in mM): 125 NaCl, 25 NaHCO3, 1.25 KCl, 1.25 KH2PO4, 1 CaCl2, 1.5 MgCl2, and 16 D-glucose, saturated with 95% O2 and 5% CO_2 (pH 7.4). The hippocampi were dissected from the rest of the brain and divided into 300 μm-thickness slices.

The establishment of different metabolic conditions was ensured upon the measurement of glycaemia levels (mg/dl) using a glucose meter (Freestyle Lite, Blood Glucose Test, Abbot®), as follows: 121.17 ± 5.73 and 44.091 ± 2.46, for fed and fasted neurones, respectively.

This paper concerns results obtained in a total of 59 rats, of which 29 were fed and 30 were kept in fasting conditions. The distribution of animals for each condition and technique used in this study was as follows (Fed; Fasted): Whole-cell (13; 16); single-channel (7; 5); Mass spectrometry (3; 3); and western blotting (6; 6).

2.3 | Cell preparation

Hippocampal pyramidal cells from the mid-third CA1 region of rats were isolated as described before (Costa, Santos, & Ribeiro, 1994). Sub-slices of the CA1 region were incubated at 32°C in an oxygen saturated solution under moderate stirring; the composition of the incubating solution was as follows (in mM): NaCl 120, KCl 5, CaCl2 1, MgCl2 1, 1,4-Piperazinediethanesulfonic acid (PIPES) 20, D-Glucose 25, adjusted to pH 7 with 1 mM NaOH. Trypsin (Sigma Type XI, 0.9 mg/ml) was added to this solution shortly after the preparation of the sub-slices; incubation period was 30–50 min, depending on rat's age. Sub-slices were transferred to an oxygen saturated enzyme-free solution after a brief wash with this solution and kept at room temperature at moderate stirring; the preparation remained viable for about 5–6 hr. Cells from the CA1 layer were isolated by gentle trituration of the sub-slices using fire polished Pasteur pipettes (1.5–2 mm bore) and dispersed in the final bath solution for electrophysiological measurements. The 35 mm plastic Petri dishes were used as recording chambers for acutely isolated cells.

2.4 | Whole-cell voltage clamp Na^+ recordings

Cells were superfused (2–3 ml/min) with an extracellular solution adequate for the recording of voltage-gated Na^+ currents. It contained (in mM): NaCI 100, KCl 5, HEPES 10 (NaOH), $CaCl_2$ 1.8, $MgCl_2$ 1, tetraethylammonium chloride (TEA-Cl) 30, $CoCl_2$ 2, 4-amino-pyridine 3, glucose 25 (pH 7.4). TEA-Cl and 4-aminopyridine were used to block potassium currents and $CoCl_2$ to block calcium currents. Osmolarity was set to 300-310 mOsm. Patch pipettes (1.5–3 MΩ), pulled from borosilicate glass (Science Products GmbH, GB150T-8P), were filled with pipette solution containing (in mM): CsF 140, NaC1 10, HEPES 10 (CsOH), EGTA 5 (pH 7.2). Osmolarity was 285-295 mOsm.

Currents were recorded with an Axopatch1D electrometer (Axon Instruments) and a pCLAMP 6.0 software (Axon Instruments). Signal was digitized using a DigiData 1200 interface and a 20 μs sampling interval. The holding potential was −70 mV. Series resistance (Rs) was compensated to about 80%–90%. The currents were sampled with a low-pass 4-pole Bessel filter at a frequency of 5 kHz. Electrode and cell membrane capacitances were compensated, and membrane surface area was estimated from the reading of the cell capacitance compensation dial, assuming a specific membrane capacitance of 1 $\mu F/cm^2$. Leak subtraction was digitally applied to raw data using a P/4 protocol (Bezanilla & Armstrong, 1977).

Patch pipettes were positioned over the soma of cells, whose selection was based on their shape and appearance: pyramidal or fusiform cell shapes (cell body length about 20-40 μm) attached to the floor of the petri dish with shinny smooth surfaces and no visible nucleus under ordinary inverted microscope optics (Olympus CK2 microscope) were preferred, the latter conditions being an indication of viability (Kay & Wong, 1986). Criteria to accept a well voltage-clamped cell were based on the pattern of current arousal (Costa et al., 1994; Sah, Gibb, & Gage, 1988): on applying depolarizing series of command pulses to the membrane, currents were evoked progressively; current records showed no delay in respect to the beginning of the command pulse and rose smoothly; current breakthrough or discontinuities were not apparent in *I–V* curves. Cells that did not comply to the above criteria were discarded. Recordings were allowed to stabilize for 5 min before current recording started, remaining stable for at least 30 min. After attaining whole cell configuration, cells were lifted from the bottom of the chamber, brought near the surface and remained under continuous bath perfusion. Experiments were carried out at room temperature (about 20°C). The junction potential for the filling and bath solution combination presently used is 9.5 mV (JPCalc, Barry, 1994). Data in the present report were not corrected for the junction potential.

2.5 | Single channel Na^+ recordings

Na^+ channel current traces were recorded using an inside-out excised patch configuration (Hamill, Marty, Neher,

Sakmann, & Sigworth, 1981), as described previously (Fernandes, Marvão, Santos, & Costa, 2001). The composition of the bath solution was as follows (mM): NaCl 0.1, CsF 145, CsCl 20, EGTA 5, and HEPES 10 (pH 7.2, CsOH); osmolarity was 320 mOsm. The pipette filling solution had the following composition (mM): NaCl 150, KCl 5, HEPES 10, $CaCl_2$ 1.8, and $MgCl_2$ 0.8 (pH 7.4, CsOH). Osmolarity was 305 mOsm. The junction potential for the filling and bath solution combination is 8.7 mV. No correction was applied for junction potential.

Micropipettes were prepared from filamented borosilicate glass capillaries (Science Products GB150F-8P), sylgarded to the tip (Dow Corning), and fire-polished to a final resistance of 15–25 MΩ. Micropipettes (final length of about 3 cm) were filled with recording solution only to the shank and back-filled with liquid paraffin (Sakmann & Neher, 1995). Noise was typically between 0.18 and 0.3 pA r.m.s. Unstable and noisy (>0.40 pA) patches were discarded. Seals resistance ranged from 20 to 100 GΩ, being often greater than 50 GΩ. Single-channel currents were recorded at 20°C with an Axopatch-200B electrometer and pClamp 6.0 software (Axon Instruments). The acquisition was made through an interface TL-1 DMA (Axon Instruments) with a sampling interval of 25 μs and analogue filtering of filter $f_a = 5$ kHz (−3 dB, 4 pole Bessel). Holding potential was −70 mV. Currents were evoked with 40 ms depolarizing command pulses ranging from −60 to +20 mV (in 10 mV steps), preceded by pre-pulses to-110 mV. Typically, patches were stable for about 30 min, occasionally for 1 hr. Capacitance transients were averaged from blank traces and subtracted to sweeps with channel openings.

The signal processing was carried out under the operator′s constant surveillance, to reduce the introduction of artefacts and to allow for event detection interpretation. Unitary Na^+ current amplitude measurements were performed using the 50% crossing method (Ogden, 1994). The rise time (t_r) is described as the time taken for the signal to rise from 10% to 90% of its final amplitude:

$$t_r = \frac{0.3321}{f_c} \quad (1)$$

where f_c is the cut-off frequency (Hz), here only characterized by the analogue filter of the recording system, 5 kHz, as no digital filtering was used. To assure the detection of fully resolved openings, an open time resolution, which is thought as the shortest time interval that can be measured, was imposed prior to histogram binning. To obtain reliable amplitude measurements, the imposed time resolution was $2\,t_r$. Thus, the maximum time resolution used in this study was 132.8 μs.

All-point amplitude histograms were constructed. The peak current of the openings was determined from Gaussian fits to the distributions (Sakmann & Neher, 1995). Channel conductance was estimated by averaging the slope of the regression line of the *I–V* plots obtained for each patch, either in fed and fasted animals.

The selection of cells followed the same criteria as above, for whole-cell experiments.

2.6 | Sample preparation for mass spectrometry

Whole-cell lysates of the hippocampus of three fed and three fasted animals were obtained by using a lysis buffer containing 150 mM NaCl, 1 mM EGTA, 50 mM Tris HCl (pH 7.4), 1% (w/v) sodium deoxycholate (D.O.C), 1% (w/v) nonidet P (NP-40), 0.1% (w/v) sodium dodecyl sulphate (SDS), 1× protease inhibitor cocktail. After sonication, samples were cleared by centrifugation at 20,000 *g* for 20 min. Protein concentration was estimated by a BCA protein assay. Reduction was done with 5 mM Ammonium bicarbonate and dithiothreitol (DTT) at 55°C for 30 min followed by alkylation with 10 mM Iodoacetamide for 30 min in dark. Proteins were then digested into peptides by LysC (Protein-enzyme ratio 1:50) at 37°C for 4 hr and trypsin (Protein-enzyme ratio 1:50) at 37°C for 16 hr according to the standard filter-aided sample preparation protocol (Wiśniewski, Zougman, Nagaraj, & Mann, 2009). Peptides were then desalted using C18 solid phase extraction cartridges (Waters) and labelled on column using stable isotope triplex dimethyl labelling on column (Boersema, Raijmakers, Lemeer, Mohammed, & Heck, 2009). Peptides belonging to fed samples were labelled with a mixture of formaldehyde and sodium cyanoborohydride ("light" reagent). For the peptides corresponding to the fasted rats, D-formaldehyde with cyanoborohydride ("medium" reagent) was used. "Light" and "medium" labelled samples were then mixed in a 1:1 ratio based on LC-MS base peak intensity. The mix was then dried in a vacuum concentrator and reconstituted in 10% formic acid for subsequent fractionation.

2.7 | Peptide fractionation

To reduce the sample complexity prior to the MS analysis, labelled peptides were fractionated using strong cation exchange chromatography (SCX). Briefly, an Agilent 1100 HPLC system (Agilent Technologies, Waldbronn, Germany) was used with a C18 Opti-Lynx (Optimized Technologies, Oregon, OR, USA) trapping cartridge and a Zorbax BioSCX-Series II column (0.8 mm × 50 mm, 3.5 μm). Labelled peptides were loaded onto the trap column at 100 μl/min and eluted onto the SCX column with 80% acetonitrile and 0.05% FA. SCX solvent A consisted of 0.05% formic acid in 20% acetonitrile and solvent B consisted of 0.05% formic acid and 0.5 M NaCl in 20% acetonitrile. We used the following gradient: 0–0.01 min (0%–2%B); 0.01–8.01 min (2%–3% B); 8.01–14.01 min

(3%–8%); 14.01–28 min (8%–20% B); 28–38 min (20%–40% B); 38–48 min (40%–90% B); 48–54 min (90% B); 54–60 min (0% B). Multiple fractions were dried in a vacuum centrifuge, reconstituted in 10% formic acid/5% DMSO prior to MS analysis.

2.8 | Mass spectrometry analysis

SCX fractions were analysed using Q-Exactive mass spectrometer (Thermo Fisher Scientific, Bremen, Germany) coupled to UHPLC Proxeon system (Easy-nLC 1000, Thermo Scientific, Odense, DK). Peptides were first loaded on a trapping column (packed in-house, Reprosil C18, 3 µm, 2 cm × 100 µm, Dr. Maisch) and then on an analytical column (packed in-house, Poroshell 120 EC-C18, 3 µm, 50 cm × 50 µm, Agilent Technologies, Netherlands). Mass spectrometry solvent A consisted of 0.1 M acetic acid in water and solvent B consisted of 0.1 M acetic acid in 80% acetonitrile. Peptides were trapped at 800 bars with 30 µl of solvent A and then loaded in the analytical column at 100 nl/min with a 60 min linear gradient from 7%–30% solvent B. Electrospray voltage of 1.7 kV was applied to the needle. The mass spectrometry was operated in the data-dependent acquisition mode and was configured to perform a survey scan from 350–1,500 *m*/*z* (resolution 7,500) followed by higher collision energy dissociation (HCD) fragmentation of the 10 most abundant peptides (32% normalized collision energy).

2.9 | Mass spectrometry data analysis

Mass spectrometry raw data were processed with MaxQuant (version 1.5.2.8; Cox et al., 2009). The database search was performed against the Rattus Norvegicus Ensemble database (version 2015_03) and Andromeda as a search engine. The following parameters were used: Carbamidomethylation (C) was set to fixed modification, oxidation (M) and demethylation (light and medium) of lysine residues and peptide N-termini were set to dynamic modification. Trypsin digestion allowing a maximum of two missed cleavages. Filtering was done at 1% false discovery rate (FDR) at the protein and peptide level. Perseus (version 1.3.0.4) was used for further analyses. Log2 transformed ratios from fed and fasted rat samples were quantified in three biological replicates. *T*-test revealed 171 proteins to be significantly enriched.

2.10 | Sample preparation for western blotting

2.10.1 | Whole-cell lysates

After dissection, the hippocampus of fed and fasted animals were immediately placed in ice-cold homogenization buffer (HB) containing (in mM): EDTA 1, Tris 50, NaCl 150 (pH7.4), and a protease inhibitor cocktail (PIC, ROCHE®, Basel, Switzerland, according to the manufacturer instructions) at the proportion of 10 mg of tissue to 100 µl of HB+PIC and stored at −80°C until required to processing. Samples were homogenized with a manual homogenizer and incubated on ice for 35 min with lysis buffer (LB): 1% (w/v) sodium deoxycholate (DOC), 1% (w/v) nonidet P-40, and 0.1% (w/v) sodium dodecyl sulphate (SDS). The lysate was centrifuged for 30 min at 13,845 *g* at 4°C and the supernatant was collected. The total protein content was determined by the bicinchoninic acid (BCA) protein assay kit (Micro BCA Pierce Thermo®, 23235) using BSA as a standard. Whole-cell lysate extracts were then immediately used or stored at −80°C until use. All steps were performed on ice and centrifugation at 4°C.

2.10.2 | Plasma membrane-enriched fractions

Hippocampal plasma membrane fractions were prepared as described previously (Sun, Huang, Kelleher, Stubbs, & Sun, 1988) with some modifications. Briefly, hippocampi from fed and fasted rats were homogenized in ice-cold homogenization buffer – 0.32 M sucrose, 50 mM Tris HCl (pH7.4), 1 mM EDTA, 2 mM EGTA, 1× protease inhibitor cocktail from Roche® Diagnostics -, using a glass tissue homogenizer pestle, and centrifuged for 10 min at 500 *g* to sediment nucleus and cell debris. The supernatant was centrifuged at 18,800 *g*, for 20 min, to obtain a crude mitochondrial pellet. The post-mitochondrial supernatant was centrifuged at 43,500 g for 30 min, which resulted in the sedimentation of a white-coloured pellet. This pellet, constituted by the crude plasma membranes, was resuspended in lysis buffer – 150 mM NaCl, 1 mM EGTA, 50 mM Tris HCl (pH7.4), 1% (w/v) sodium deoxycholate (D.O.C), 1% (w/v) nonidet P (NP-40), 0.1% (w/v) sodium dodecyl sulphate (SDS), 1× protease inhibitor cocktail– and placed on ice for 30 min. The protein concentration was determined by the bicinchoninic acid (BCA) protein assay kit (Micro BCA Pierce Thermo®, 23235) using BSA as a standard. Plasma membrane-enriched fractions were then immediately used or stored at −80°C until use. All steps were performed on ice and centrifugations at 4°C.

2.11 | Western blotting

Twenty microgram proteins were denaturated in Laemmli sample buffer containing (in %w/v): dithiothreitol (DTT) 0.77, bromophenol blue 0.01, glycerol 5, SDS 1.5, and Tris-HCl 0.5M (pH 6.8); applied in a 7% SDS-Polyacrylamide gel electrophoresis and wet transferred to a Polyvinylidene difluoride (PVDF) membrane. Blots were blocked for 2 hr at room temperature in 5% skimmed milk in Tris-buffered saline (TBS) with 0.1% of Tween 20 detergent (TBS-T 0.1%)

prior to the incubation with primary antibody overnight at 4°C. The antibodies used were polyclonal anti-Nav1.2 (1:1,000, Alomone labs®, ASC-002) and as a loading controls, the monoclonal anti-alpha Tubulin (1:2,000, Santa Cruz®, SC 58666) and polyclonal anti N-cadherin (1:1,000, Alomone labs®, ANR-082), for whole-cell lysates and plasma membrane samples, respectively. Blots were washed several times in TBS-T 0.1% and incubated with the secondary antibody polyclonal goat anti-rabbit IgG (H&L) peroxidase conjugated (1:3,000, Rockland®, 611-1302) for 120 min at room temperature. Membranes were washed in TBS-T 0.1% and incubated with enhanced luminol chemiluminescence reagents (Clarity ECL Bio-rad®) according to the manufacturer instructions. The density of the signals was detected in a Chemidoc Molecular Imager (Chemidoc, Biorad®) and densitometry was performed using the ImageLab software (Biorad®).

2.12 | Statistical analysis

Statistical analyses were performed using SigmaStat 4.0 (Systat Software, Inc., San Jose, CA, USA). The significance of the differences between the data of the two groups studied – fed and fasted animals – was calculated as follows: Samples size $n \geq 10$ were subjected to a two-tailed unpaired student's t test; samples in which $n < 10$ or that failed normality test, the non-parametric Mann–Whitney U-test was used for statistical procedures. Values given in the text are means ± SEM, unless otherwise stated. Differences in experimental data were considered statistically significant for $p < 0.05$.

Off-line analysis of electrophysiological data was carried out using Clampfit 10 (Molecular Devices, USA), Origin 8.0 (Originlab, USA), and Microsoft Excel® (Microsoft, USA).

3 | RESULTS

3.1 | Whole-cell voltage clamp analysis

3.1.1 | Voltage dependence of activation

Recordings from CA1 hippocampal neurones showed the common behaviour of Na^+ currents (Figure 1), with a fast activation and a spontaneously rapid decay (Bruehl & Witte,

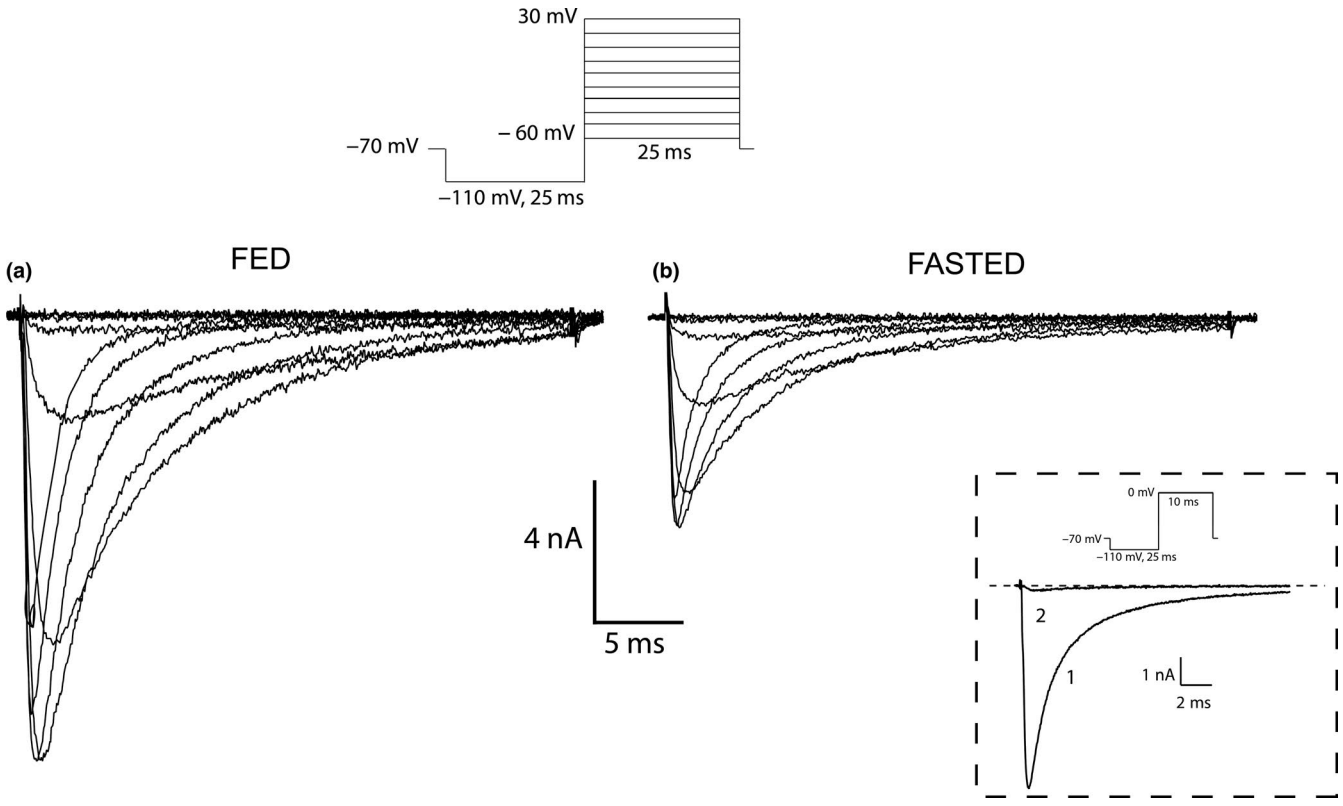

FIGURE 1 Effect of feeding cycle over the whole cell Na^+ currents of acutely isolated rat CA1 hippocampal neurones. Representative whole-cell voltage clamp Na^+ currents, recorded in patches from fed (a) and fasted (b) animals, were evoked in series of depolarization command pulses (25 ms in duration), in steps of 10 mV, from −60 mV to +30 mV, following a hyperpolarizing conditioning pulse at −110 mV (25 ms in duration). Holding potential was set at −70 mV. Traces depict increased Na^+ current amplitude in fed animals. The inset confirms the nature of the currents, as trace 1 (control current) was blocked by 1 μM TTX application (trace 2); currents evoked with a command potential to 0 mV from a −110 mV pre-pulse, with a holding potential of −70 mV

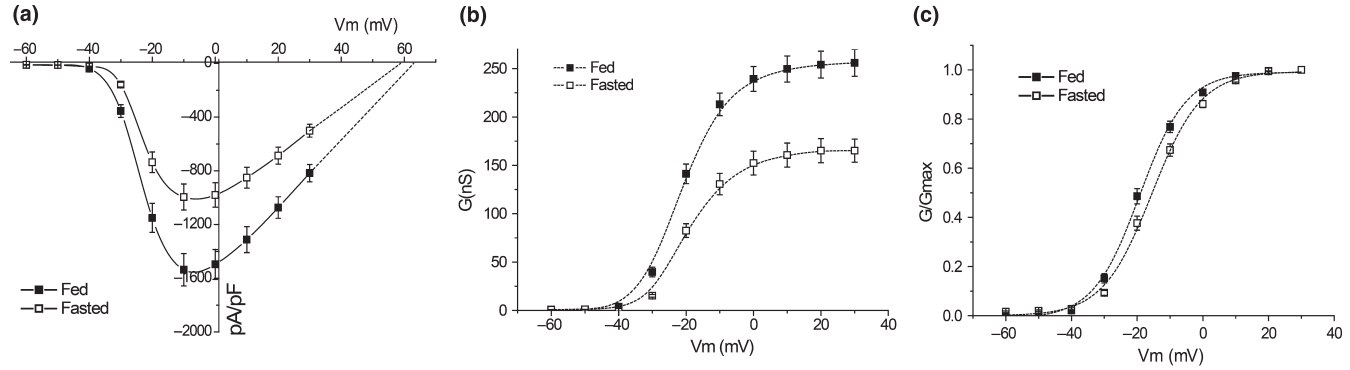

FIGURE 2 Influence of feeding cycle on the voltage dependence of activation of Na^+ currents. Activation curves relate to Na^+ currents like those depicted in figure 1. (a) *I–V* curves related to mean peak Na^+ current normalized to cell capacitance (pA/pF); (b) Mean conductance (*G*(nS)) of peak Na^+ currents; and (c) mean conductance normalized to the maximum value (G/G_{max}), obtained from freshly isolated rat hippocampal CA1 neurones of fed (filled squares; $n = 18$) and fasted (open squares; $n = 28$) animals. Dashed lines in (b) and (c) are the solution of Equation 3 (in C, $V_h = -19.2$ mV and $V_s = 7.1$ mV/e-fold, for fed neurones; $V_h = -15.5$ mV and $V_s = 7.5$ mV/e-fold, for fasted neurones). Error bars are ±*SEM* values

2003; Costa, 1996; Ketelaars, Gorter, van Vliet, Lopes da Silva, & Wadman, 2001; Sah et al., 1988; Vreugdenhil, Faas, & Wadman, 1998), reaching a peak within 0.6 ms at −10 mV. Na^+ currents were evoked with a step of depolarized voltages from −60 mV up to +30 mV, following a conditioning pulse of −110 mV, with a duration of 25 ms, to remove inactivation. Holding potential was set at −70 mV.

The conspicuous effect of feeding cycle on Na^+ currents is depicted in Figure 1, which illustrates representative recordings assigned to fed and fasted neurones. Na^+ current amplitude increased upon feeding, as depicted in the current to voltage (*I–V*) relationship, whose data comprise the mean peak Na current values obtained in the voltage range studied (−60 mV to +30 mV; Figure 2). Peak current values, I (pA), were normalized to cell capacitance (pA/pF), as a measure of the current density (Figure 2a).

One might estimate that the average maximum current density (assuming 1 μF corresponds to 1/cm^2, Hodgkin and Huxley) for fed and fasted neurones, at −10 mV, was 1.5 mA/cm^2 ± 0.12 ($n = 18$) and 1.0 mA/cm^2 ± 0.10 ($n = 28$), respectively. The difference is statistically significant ($p = 0.0009$). Furthermore, the reversal potential measured by linear extrapolation was close to the theoretical equilibrium potential for Na^+ ions of +57.6 mV, predicted by the ionic conditions. This result, together with the blockade of Na^+ currents by TTX (see inset in Figure 1), accounts for the involvement of Na^+ currents towards the influence of feeding cycle on rat hippocampal CA1 neurones activity.

Peak current values were also converted to conductance, *G*(nS), as follows:

$$G = I/(V_m - E_{Na^+}) \quad (2)$$

where *I* is the current amplitude, V_m is the step command potential, and $E_{Na}+$ is the estimated equilibrium potential for Na^+.

Fed neurones present higher values of conductance nearly in all studied voltage range (Figure 2b). At 30 mV, membrane potential at which all Na^+ channels must be open, the mean maximum conductance values were 255.9 ± 13.95 nS and 165.2 ± 11.98 nS for fed and fasted neurones, respectively. The results are statistically significant ($p < 0.0001$). Taken together, Figure 2a,b show that fed neurones exhibit higher whole cell Na^+ current density and conductance.

The voltage dependence of activation was studied normalizing *G*(nS) for its maximal value (G/G_{max}) and plotting the mean values against step command potential (Figure 2c). The analysis of the fraction of open channels was carried out by fitting a Boltzmann distribution to the resulting data, whose parameters quantify the influence of feeding cycle in the activation of Na^+ channels:

$$G/G_{max} = 1/\{1 + \exp[(V_h - V_m)/V_s]\}, \quad (3)$$

where V_h is the half-activation potential (mV), V_s is a slope factor (mV/*e*-fold), and V_m is the step command potential (mV).

The average fitting parameters values of activation curves – V_h and V_s – are presented in Table 1. V_h values were as follows: −15.2 ± 0.89 mV and −19.1 ± 0.87 mV, for fed and fasted neurones, respectively. This result is statistically significant ($p = 0.005$), supporting the shift towards hyperpolarizing potentials (roughly 4 mV) of the activation of Na^+ currents, observed in fed neurones (Figure 2c). V_s values were similar in both conditions: 6.7 ± 0.35 mV/e-fold and 6.8 ± 0.25 mV/e-fold, for fed and fasted neurones, respectively.

3.1.2 | Steady-state inactivation (h_∞)

The steady state of inactivation was studied with a conditioning double-pulse protocol (Hodgkin & Huxley, 1952),

TABLE 1 Activation and steady-state inactivation (h_∞) fitting parameters V_h (mV) and V_s (mV/e-fold) (Equation 3) for neurones of fed and fasted animals. Statistical analysis performed with a *t*-test; $0.001 < p\text{-value} < 0.01$

	Voltage dependence of activation (mV)			Voltage dependence of inactivation (mV)		
	V_h	V_s	n	V_h	V_s	n
Fed	−19.1 ± 0.87	6.7 ± 0.35	18	−51.2 ± 1.50	9.8 ± 0.45	24
Fasted	−15.2 ± 0.89	6.8 ± 0.25	28	−58.4 ± 1.81	10.9 ± 0.35	27
p-value	0.005	n.s.	–	0.004	n.s.	–

by which Na^+ currents were evoked with pre-pulses ranging from −120 mV to 0 mV, 40 ms in duration, from a holding potential of −70 mV, in conjunction with a depolarizing command step to a fixed voltage (0 mV, 30 ms). Currents evoked with such voltage-clamp protocol are depicted in Figure 3a,b.

Peak current values were normalized to the maximal response (I/I_{max}) and plotted against pre-pulse potential to obtain steady-state inactivation curves (Figure 3c). Data points were fitted with a Boltzmann distribution (Equation 3) and the results can be directly compared with the h_∞ curve obtained by Hodgkin and Huxley (Hodgkin & Huxley, 1952), giving us information about the steady state availability of sodium channels to respond to activation.

The quantification of the effect of feeding cycle over the steady state of inactivation is shown in Table 1. The average fitting parameters were as follows: $V_h = -51.2 \pm 1.50$ mV, $V_s = -9.8 \pm 0.45$ mV/e-fold in fed neurones ($n = 24$) and $V_h = -58.4 \pm 1.81$ mV, $V_s = -10.9 \pm 0.35$ mV/e-fold in fasted neurones ($n = 27$). The results demonstrate that Na^+ currents in CA1 neurones showed a significant voltage shift during the feeding cycle ($p = 0.004$). As presented in Figure 3c, from −90 mV to −40 mV, the Na^+ currents of fed animals display comparatively higher I/I_{max} values due to a shift towards depolarized potentials by 7 mV. Thus, the voltage profile observed in inactivation curves of fed neurones showed a significant depolarization in comparison with that obtained in fasted neurones. This demonstrates that Na^+ currents in fasted neurones begin to inactivate at more negative potentials. Once again, the voltage sensitivity, given by the steepness of the h_∞ curves, was similar in both conditions.

3.1.3 | Na^+ channel availability

To a better visualization of the effect of feeding cycle on the steady state properties of activation and inactivation, we have addressed the fraction of permanently activated channels. Overlapping the activation and inactivation of Na^+ channels, it is possible to define a range of voltages (i.e. "window") where the channels are partially activated but not fully inactivated (Figure 4).

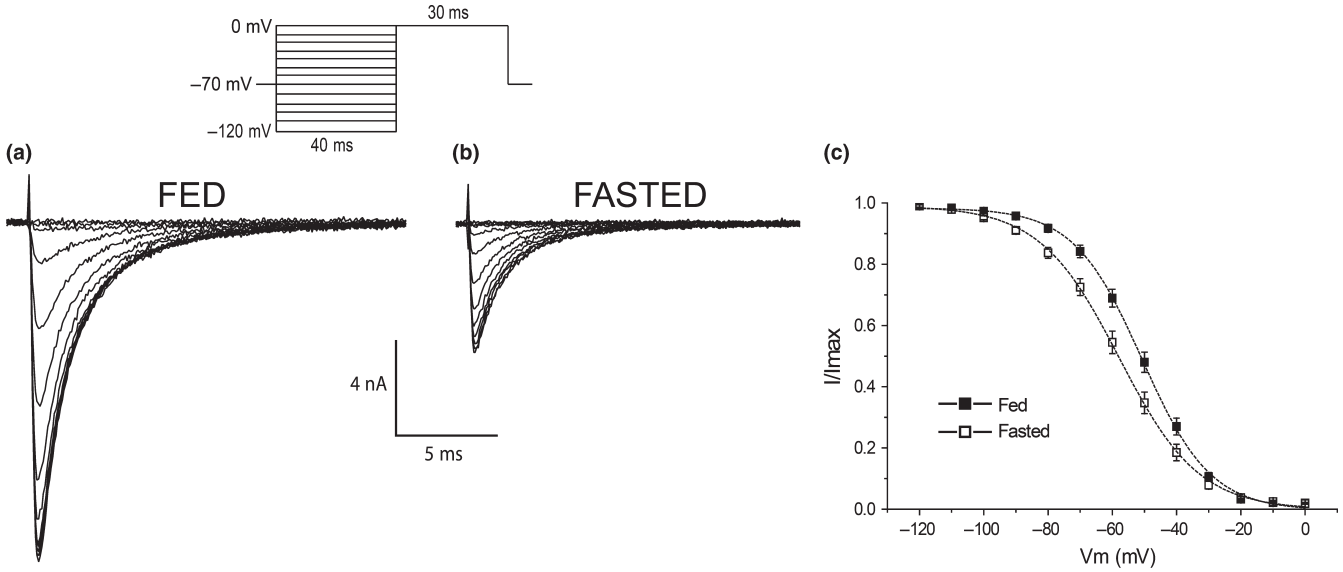

FIGURE 3 Influence of feeding cycle on steady-state inactivation (h_∞) of Na^+ currents. Whole-cell voltage clamp Na^+ currents were evoked by a command step to 0 mV (30 ms) following a set of pre-pulses (40 ms) ranging from −120 to 0 mV in steps of 10 mV; holding potential of −70 mV (inset). Records were obtained from a neuron of a fed (a) and (b) fasted animal. (c) Mean peak Na^+ current obtained in the test pulse normalized to the maximum value (I/I_{max}) as a function of pre-pulse potentials, from neurones of fed (filled squares; $n = 24$) and fasted (open squares; $n = 27$) animals. The steady-state inactivation curves (h_∞) were fitted with equation 3 ($V_h = -50.7$ mV and $V_s = 10.7$ mV/e-fold, for fed neurones; $V_h = -57.8$ mV and $V_s = 12.4$ mV/e-fold, for fasted neurones). Error bars are ±*SEM* values

The probability of being within this "window", highlighted in Figure 4a as a gray area, was calculated from the product of the activation and steady-state inactivation curves (Huang et al., 2011). Figure 4b shows that the feeding enlarged the window, shifted the peak towards negative potentials and produced a twofold increase in amplitude (~3%).

3.1.4 | Time-constant of inactivation (τ_h)

The decay phase of the Na^+ currents, obtained with activation protocols (Figure 1), was described with an exponential time course, using an equation of the form

$$I = a_f e^{-t/\tau_{hf}} + a_s e^{-t/\tau_{hs}} + C \quad (4)$$

where τ_{hf} and τ_{hs} are the time-constants of the fast and slow inactivating components, respectively; a_f and a_s are the amplitude coefficients and C is a constant.

Figure 5a illustrates exponential fits to the decay phase of currents evoked in command steps to −30, −25 and −20 mV from −70 mV holding potential. At −30 mV, the current decayed monoexponentially with a time constant of 8.1 ms; at −25 and −20 mV, the inactivating phase was best described by two exponentials, with time constants of 7.6; 3.8 ms and 6.8; 2.5 ms, respectively. Figure 5b shows the mean inactivation time constants values measured in activation protocols. At a hyperpolarized V_m range (from −45 to −30 mV), we could only determine a single exponential with slow kinetics (τ_{hslow}); at −40 mV, we have obtained τ_{hslow} 18.6 ± 2.81 ms and τ_{hslow} 11.7 ± 0.83 ms for fed and fasted neurones, respectively. Results are statistically significant ($p = 0.009$). For voltage command steps more depolarized than −25 mV, two exponentials were ascribed to the time course of inactivation, revealing the existence of two inactivating components, with slow (τ_{hslow}) and fast kinetics (τ_{hfast}). In command steps to −20 mV, the mean inactivation time constants measured in fed neurones were as follows: τ_{hslow} 8.5 ± 0.95 ms and τ_{hfast} 2.2 ± 0.24 ms. In fasted neurones, the mean inactivation time constants were: τ_{hslow} 6.6 ± 0.52 ms and τ_{hfast} 2.4 ± 0.39 ms. Overall, the effect of feeding cycle over the voltage dependence of the time-constant of inactivation is evident at more hyperpolarized potentials, between −45 mV and −20 mV.

Furthermore, as previously observed by Costa (1996), the proportion of fast and slow inactivating components—a_{fast} and a_{slow}—changed with depolarization. The faster inactivating component dominated at values less negative than −20 mV, attaining ~92% of total current amplitude at large depolarizations up to +30 mV, in fed neurones. Figure 5c depicts the voltage-dependence of the ratios calculated from the coefficients in Equation 4 (a_f/a_s). At 30 mV, the mean ratio values were: 10.3 ± 2.26 and 8.7 ± 3.25 for fed ($n = 18$) and fasted ($n = 28$) neurones, respectively. Ratio values obtained from fed and fasted neurones, in the voltage range between 10 and 30 mV, were statistically significant (at 10 mV, $p = 0.036$; at 20 mV, $p = 0.032$ and at 30 mV, $p = 0.012$). Higher a_f/a_s ratio values assigned to fed neurones suggests a greater variation on the Na^+ channel expression levels upon feeding.

3.2 | Single-channel analysis – inside-out excised patch configuration

3.2.1 | Unitary Na^+ channel currents

The macroscopic Na^+ currents showed distinct characteristics whether the animals were fed or kept in fasting conditions. To further understand the underlying mechanisms of

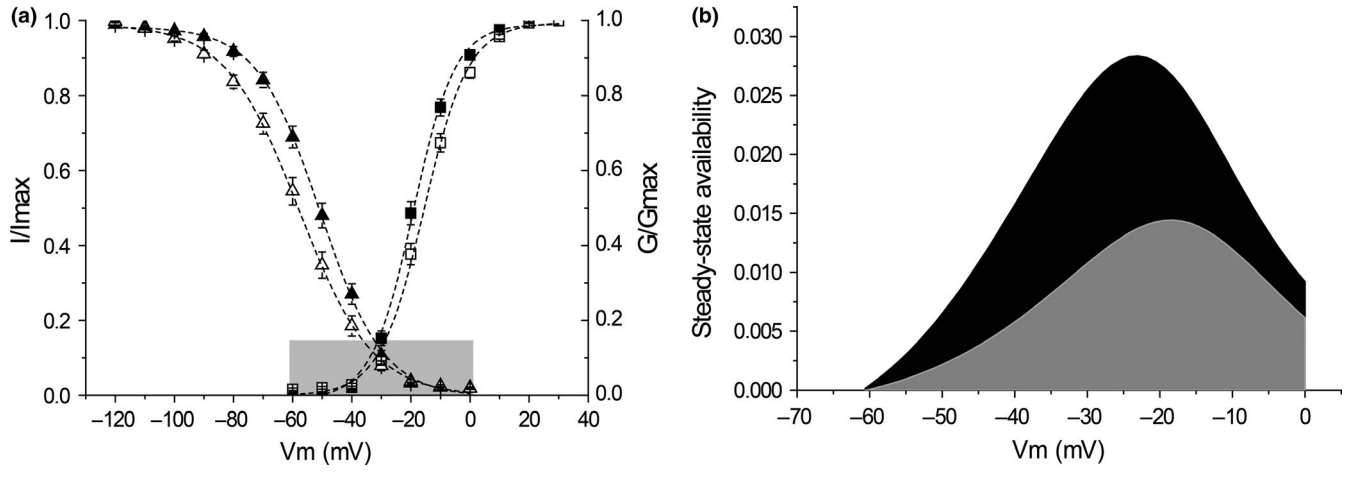

FIGURE 4 "Window current" of voltage gated Na^+ currents obtained from neurons of fed and fasted animals. (a) Voltage dependence of activation and steady-state inactivation curves as depicted in Figures 2b and 3c. The area highlighted by a grey area relates to a voltage range ("window") in which Na^+ currents are partially activated although not fully inactivated. (b) The product of the activation and h_∞ curves give the probability of channels being present in this region (Huang et al., 2011). Na^+ channels in fed animals (black area) depict a larger availability when compared to the Na^+ channels in fasted animals (grey area)

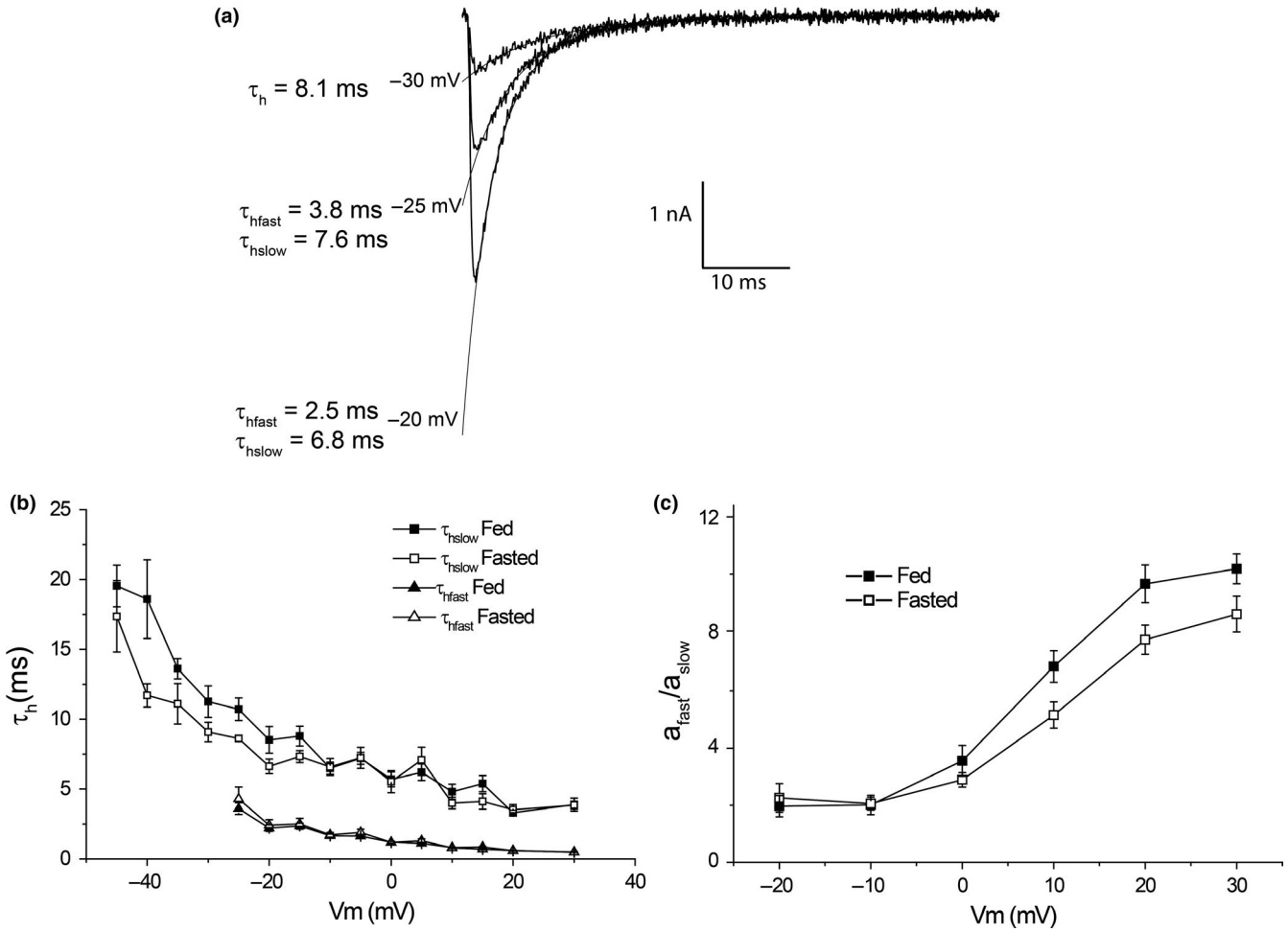

FIGURE 5 Effect of feeding cycle on the kinetics of inactivation of Na^+ channels. (a) Fitting of the decay phase of Na^+ currents evoked by an activation protocol. The inactivation could be described by a single (−30 mV command pulse) or a by double exponential (−25 and −20 mV command pulses), Equation 4. (b) Voltage-dependence of the time-constant of inactivation (τ_h(ms)) measured in activation protocols, in which Na^+ currents were evoked in series of depolarization command pulses, in steps of 5 mV, from −45 to +30 mV; slow (squares) and fast (triangles) inactivation components in neurones of fed (filled symbols; $n = 18$) and fasted (open symbols; $n = 28$) animals. (c) Voltage-dependence of the fast/slow ratio of the two exponential components of inactivation in fed (filled squares, $n = 18$) and fasted (open squares, $n = 28$) neurones. Error bars are ±*SEM*

such outcome, it was critical to address the effect of feeding cycle on the Na^+ channel functioning at a microscopic level.

Figure 6 illustrates single channel Na^+ currents in several patches of fed and fasted neurones, using an excised inside-out patch configuration. Fed neurones comprised patches with higher current amplitudes. In the patches illustrated in Figure 6 it is shown that the observed delta in current amplitude between feeding conditions was obvious at hyperpolarized V_m values, becoming negligible as the command potential steps are depolarized; at −60 mV, we could observe a clear difference in current amplitude, which was not observed at −10 mV.

3.2.2 | Amplitude measurements

The analysis of the single channel records followed the 50% threshold method (Sakmann & Neher, 1995). All point histograms were constructed from the detected events. Figure 7 depicts all-point amplitude histograms obtained in patches from fed and fasted neurones, at a pulse command step of −60 mV.

Each amplitude histogram was best described by two Gaussian distributions corresponding to the baseline current (around 0 pA, closed states) and the open-channel current, and fitted with a sum of two gaussian curves (presented as dashed lines in Figure 7a and lines in Figure 7b):

$$f(I) = \sum_{i=1}^{n} A_i \frac{e^{-(x-\mu_i)^2/(2\sigma_i^2)}}{\sigma_i\sqrt{2\pi}} + C \quad (5)$$

where μ_i is the mean value, σ_i is the standard deviation (*SD*), and A_i is the amplitude of the corresponding curves.

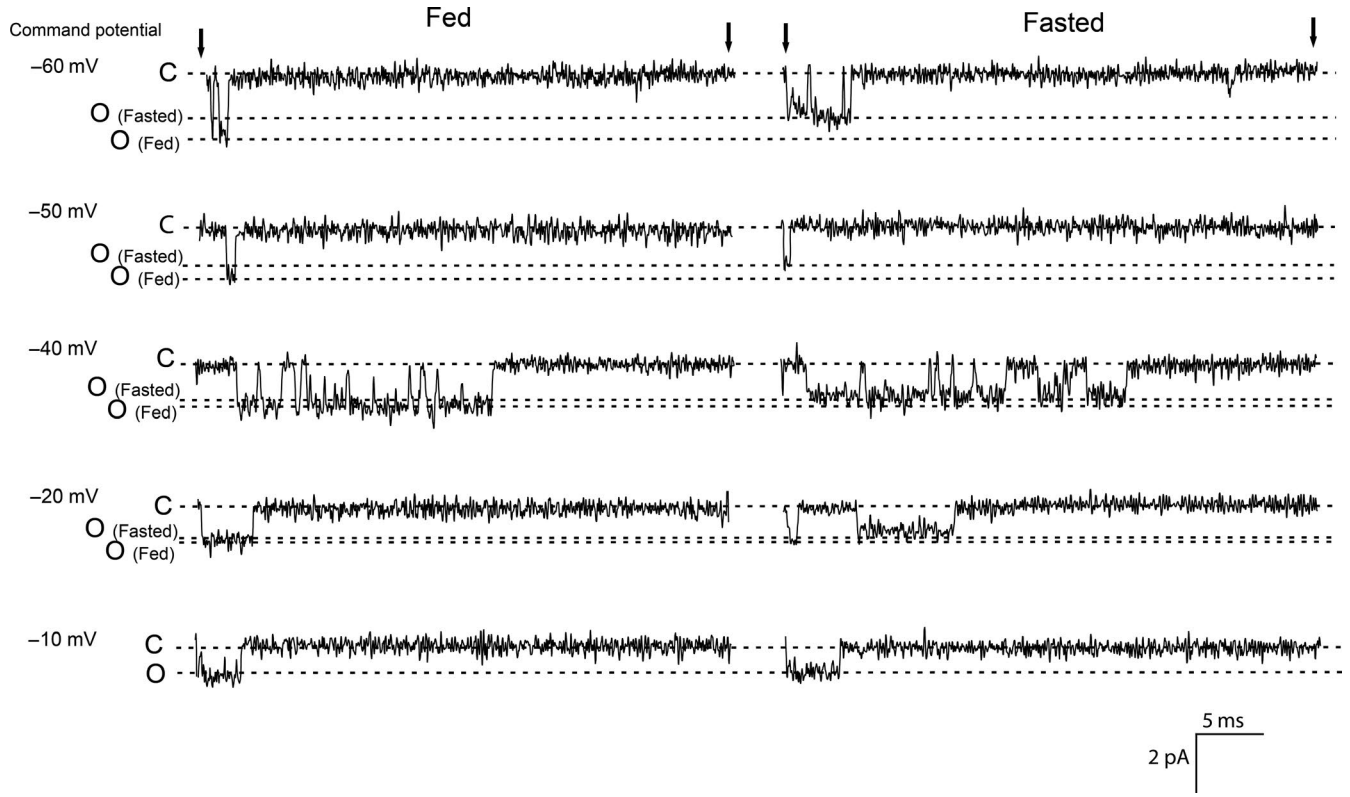

FIGURE 6 Influence of the feeding cycle on single channel Na^+ currents of acutely isolated rat hippocampal CA1 neurones. Single-channel current traces, obtained in inside-out excised configuration, in different patches from neurones of fed and fasted animals, at voltage command steps shown on the left of each record and from a holding potential of −110 mV. Arrows (↓) indicate the onset and the end of the voltage command pulses. The horizontal dashed lines represent the closed (C) and open (O) states of channels in preparations from either fasted or fed rats

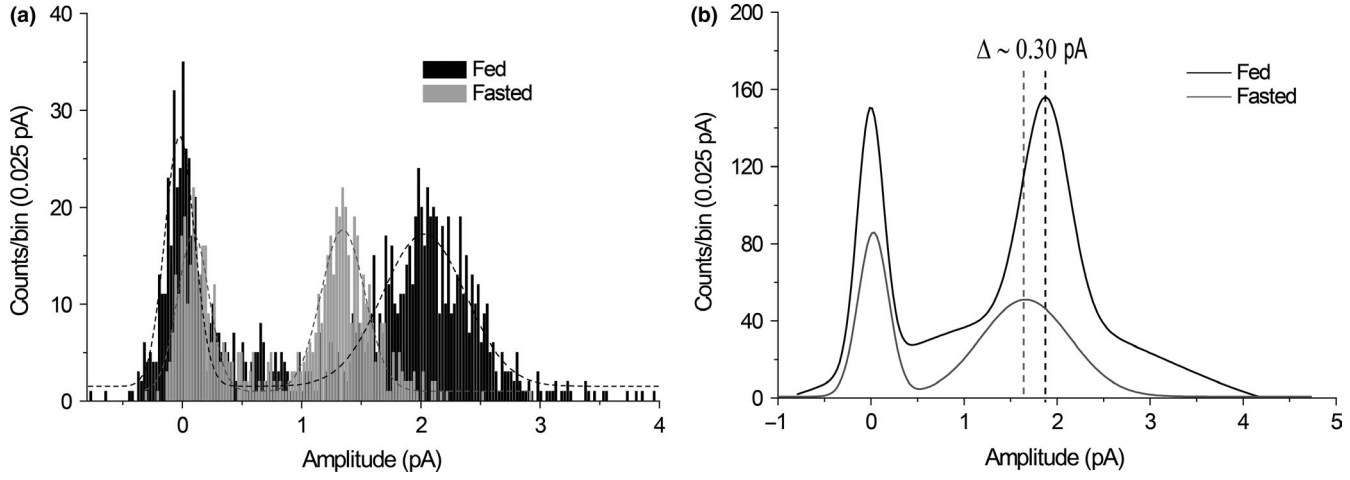

FIGURE 7 All-point amplitude histograms (APAH) of unitary Na^+ currents and corresponding Gaussian fits in patches from fed and fasted animals, at −60 mV. Single channel Na^+ events obtained by the 50% threshold method (details in Section 2). (a) APAH of two different recordings in patches from fed (black traces) and fasted (grey traces) animals. The dashed lines were obtained by fitting Equation 5 (Gaussian distribution). The humps corresponding to open events are located at peak values of 1.35 pA (fasted condition) and at 2.02 pA (fed condition). (b) Fitting Gaussian curves of pooled data from patches of fed (black line, $n = 8$) and fasted (grey line, $n = 8$) animals. The difference between the two peaks is indicated (~0.3 pA; $p = 0.038$)

The mean amplitude ($\mu \pm SD$) of patches represented in Figure 7a was estimated as -1.4 ± 0.20 pA for a fasted neuron, and -2.0 ± 0.23 pA for a fed neuron. In this example, the observed current amplitude in fasted condition was remarkably reduced. Figure 7b shows the Gaussian fitting curves related to the average of all-point histograms at −60 mV. At

this V_m, the unitary Na^+ current amplitudes (±*SEM*) were −1.9 ± 0.03 and −1.7 ± 0.09 pA for fed ($n = 8$) and fasted ($n = 8$) neurones, respectively. This result is statistically significant ($p = 0.038$) suggesting an influence of feeding cycle over the unitary conductance (see Figure 8a).

Following this rationale for all patches, we managed to analyse the amplitude of fully resolved openings obtained in voltage steps ranging from −60 to +20 mV. Figure 8a depicts Na^+ channel unitary current as a function of step command voltage (*I–V* plots) in patches from fed and fasted neurones. Points in the plots are mean values and concern measurements obtained in a total of 18 patches, nine in fed and nine in fasted conditions.

The unitary Na^+ channel conductance was estimated from the slope of the regression lines calculated in all patches studied. To obtain reliable slope results, we only used patches where at least four voltage commands were applied. The bars represented in Figure 8b are mean values. The calculated mean slope conductance for fed neurones determined between −60 and +20 mV was 16.1 ± 0.76 pS ($n = 8$). Fasted neurones disclosed a smaller mean slope conductance of 12.6 ± 1.30 pS ($n = 8$). These results are statistically significant ($p = 0.016$), confirming that each Na^+ channel present in the surface of CA1 neurones of fed animals conduct more Na^+ ions, as compared to every single Na^+ channel located in CA1 neurones of fasted animals.

3.3 | Na^+ channel expression analysis – Mass spectrometry and western blotting

We have addressed the likely involvement of the differential expression of Na^+ channel isoforms (see Figure 5c), as a further explanation to the different electrophysiological properties of Na^+ channels. The following proteomic analysis has been conducted on the entire tissue of the rat hippocampus.

3.3.1 | Mass spectrometry – proteome of the rat hippocampus

The proteome of the rat hippocampus was analysed by LC-MS/MS analysis, in whole-cell lysates of three fed and three fasted animals. Using dimethyl labelling (Boersema et al., 2009) coupled with LTQ-Orbitrap mass spectrometer, a total of 4,925 proteins were identified. The subcellular locations of the identified proteins were categorized according to the universal Gene Ontology cellular component annotation (http://geneontology.org/). Of the proteins classified as voltage-gated protein ion channels, only three were assigned to the category of voltage-gated sodium channels. Table 2 indicates that Nav1.2 was the only functional alpha subunit detected in the rat hippocampus, along with the presence of two modulatory beta subunits—beta 2 and beta 4.

The impact of feeding cycle on the protein expression was analysed. The Volcano plot of proteomics data (Figure 9) depicts protein data *p*-values vs. log2 fold change (fasted/fed).

Most of the proteins quantified did not disclose significant expression differences in response to feeding cycle (grey dots in Figure 9, *p*-value >0.05, $n = 3$). In total, only 171 of the 4,925 proteins identified were found to be differently expressed throughout the feeding cycle: 120 were up-regulated (filled black circles) and 51 were down-regulated (open black circles). Conversely, Nav1.2 channel fits within the range of proteins whose expression changes are not statistically significant between fed and fasted samples (cross mark in Figure 9;

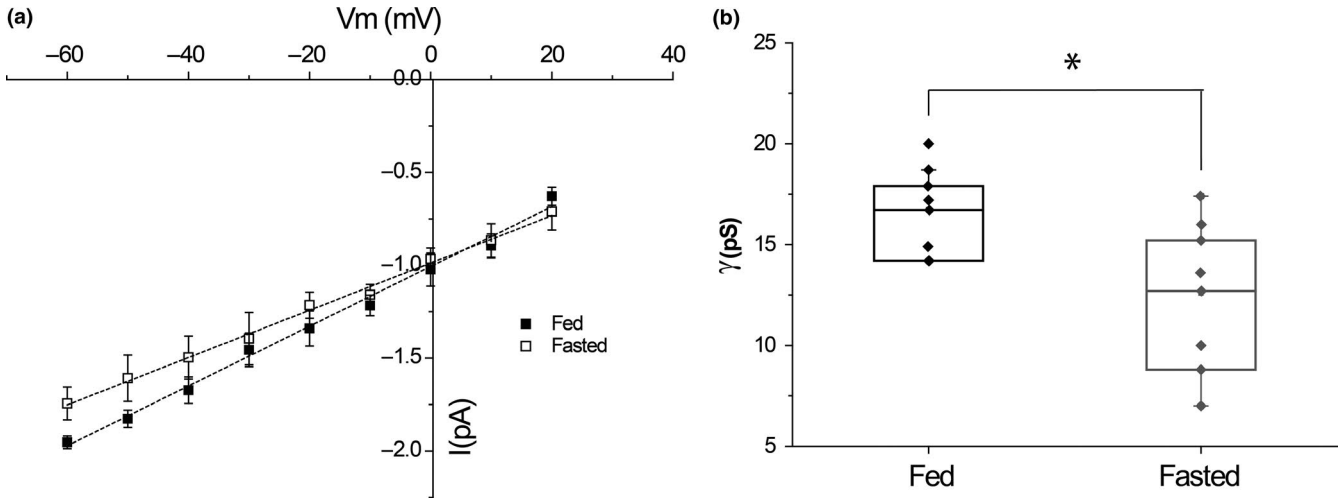

FIGURE 8 Single channel Na^+ slope conductance determined by linear regression of *I–V* data. (a) Mean single channel current amplitude was accessed in fully resolved openings and determined by fitting all-points histograms (see Figure 7) in patches from fed ($n = 9$ patches) and fasted ($n = 9$ patches) neurones, in voltage command steps from −60 to +20 mV. Dashed lines are linear regression of the average data. (b) Mean single-channel slope conductance, γ(pS), of patches from fed (~16.7 ± 0.76 pS, $n = 8$) and fasted (~12.6 ± 1.30 pS, $n = 8$) neurones. Error bars are ±*SEM* (*t*-student analysis; $p = 0.016$)

TABLE 2 Profiling of Voltage-gated sodium channels in the rat hippocampus proteome

Category	Protein IDs	Protein/gene name
Voltage-gated Sodium channels	Q7M730	Sodium channel subunit beta-4/Scn4b
	P54900	Sodium channel subunit beta-2/Scn2b
	P04775	Sodium channel protein type 2 subunit alpha/Scn2a

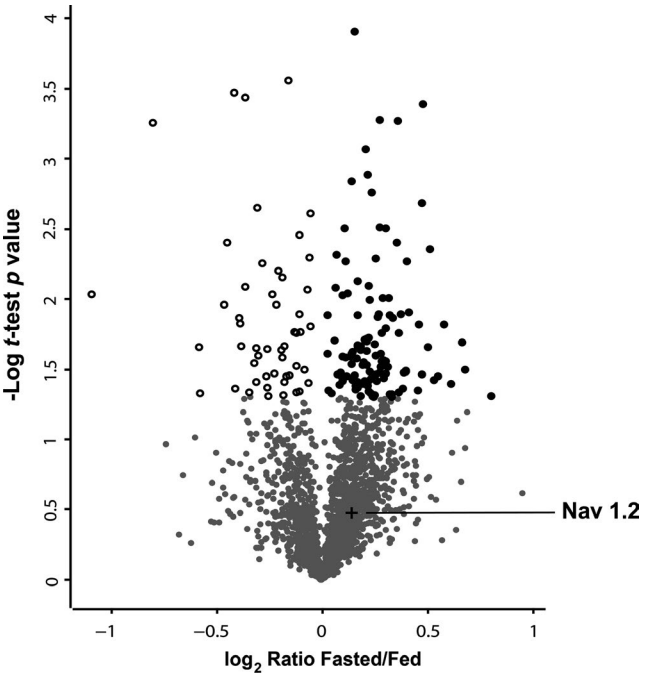

FIGURE 9 Regulation of the rat hippocampus proteome throughout the feeding cycle. Volcano plot illustrates the distribution of all proteins commonly quantified in fed and fasted samples obtained from whole cell extracts of rat hippocampus ($n = 6$; three fed and three fasted). The *x*-axis represents the average log2 fold change (fasted/fed). The *y*-axis represents the −log *t*-test (*p*-value). Filled and open black circles refer to significantly up- and down-regulated proteins, respectively (significance <0.05). The highlighted cross mark within the range of non-regulated proteins (grey dots) indicates the protein expression change of Nav 1.2 channel

$p = 0.47$, $n = 3$). This is consistent with a steady gene expression regulation of Nav1.2 throughout the feeding cycle.

3.3.2 | Western blotting—$Na_v1.2$ expression in whole-cell lysate and membranes

Western blotting experiments were conducted to address the expression of $Na_v1.2$ in two groups of rat hippocampal samples, based on the nature of the protein extraction methods: whole-cell lysates and plasma membrane-enriched fractions. Each group comprises samples obtained from three fed and three fasted animals (see Section 2). Our goal was to compare the impact of feeding cycle on the $Na_v1.2$ channel density in the whole hippocampus and at the plasma membrane of hippocampal cells, where they are functionally active.

Figure 10 illustrates the impact of fed and fasted conditions on the Nav1.2 channel density. In whole-cell lysates (Figure 10a), there was no significant variation in Nav1.2 levels during the feeding cycle, as indicated by the quantitative analysis (Figure $10a_{ii}$; $p = 0.67$). This corroborates well with the LC-MS/MS results. Contrastingly, in plasma membrane-enriched fractions (Figure 10b), we observed higher levels of Nav1.2 expression in samples obtained from fed animals. This variation is statistically significant ($p = 0.041$; Figure $10b_{ii}$). These results strongly suggest that the impact of feeding cycle on the $Na_v1.2$ density is confined to the plasma membrane of hippocampal cells, as no difference has been revealed when we considered all cell structures (whole-cell lysate samples).

4 | DISCUSSION

This study aimed at providing data concerning the effect of feeding cycle on sodium (Na^+) currents (I_{Na}) in acutely isolated rat hippocampal CA1 neurones. For such, we developed an integrated analysis of the biophysical and biochemical properties of I_{Na} in neurones of fed and fasted animals.

The significant differences between fed and fasted neurones can be summarized as follows: in fed neurones, the whole-cell currents showed (a) a 1.5-fold increase in average maximum current density values; (b) a hyperpolarizing shift in the voltage dependence of activation curves and a depolarizing shift in the voltage dependence of both (c) steady-state inactivation (h_∞) curve and (d) time-constant of the slow inactivating component (τ_{hslow}). Also, in fed neurones, single-channel current recordings displayed (e) higher Na^+ channel unitary current amplitudes and (f) larger conductance mediated through single channels. Finally, western blotting results disclosed (g) an increase in the concentration of a specific Na^+ channel α-subunit, $Na_v1.2$, in plasma membrane-enriched fractions of the hippocampal cells of fed animals (but not in whole-hippocampus preparations) and (h) proteomic analysis showed that the alterations seen are not due to changes in protein synthesis.

Considering the voltage dependence of activation curves of I_{Na} obtained from both conditioned neurones, mean V_h values were significantly different, with fed neurones depicting a hyperpolarizing shift (about 4 mV) in comparison to fasted neurones (see Table 1). This result indicates an influence of feeding cycle on the conductance of the Na^+ channel population of rat hippocampal CA1 neurones, suggesting a facilitation of the activation process in fed neurones. More specifically, upon feeding, there must be more Na^+ channels

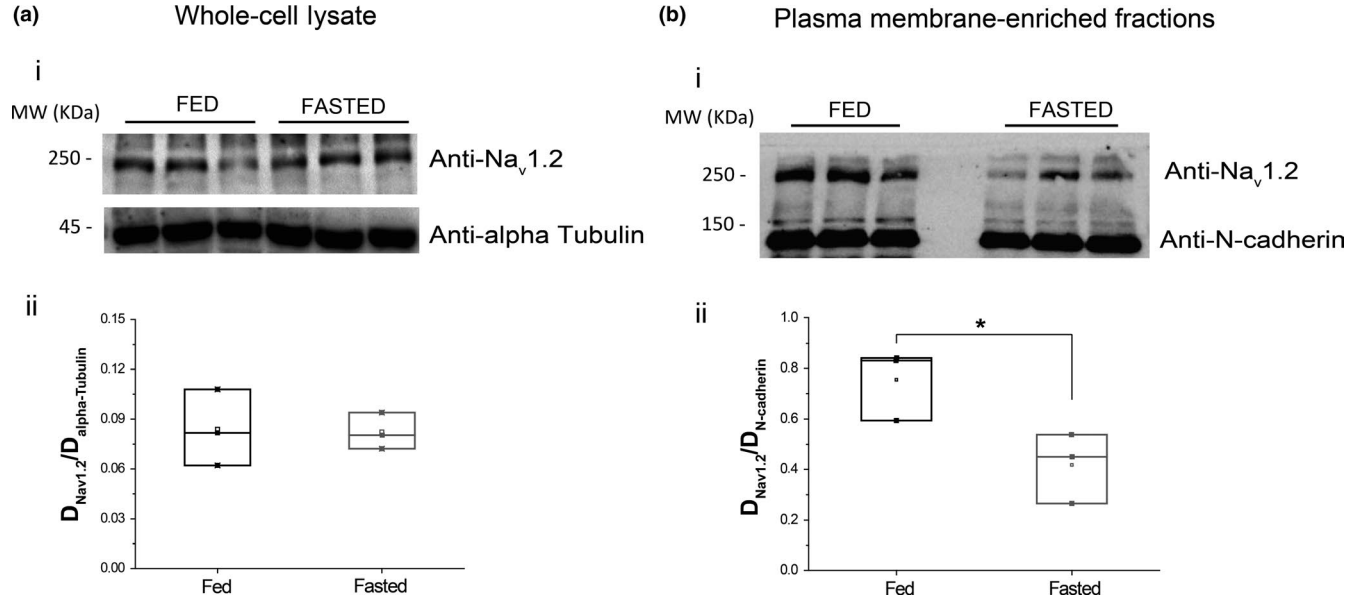

FIGURE 10 Expression of rat brain Na^+ channel subtype $Na_v1.2$ in whole cell lysate extracts and plasma membrane-enriched fractions sampled from the hippocampus of fed and fasted rats. Western blotting PVDF membrane of whole cell lysate extracts (a_i) was marked with antibody raised against $Na_v1.2$ (1:2,000) and alpha-Tubulin (1:2,000), as a loading control. The membrane corresponding to membrane fractions (b_i) was marked with anti-Nav1.2 and anti N-cadherin (1:1,000), as loading control. In both membranes, the first three lanes, on the left, correspond to fed samples and the last three, on the right, to fasted samples. Densitometry results assigned to whole cell extracts (a_{ii}) and membrane fractions (b_{ii}) were obtained by dividing the blot areas measured in ImageLab software (Biorad®). The results expressed in b_{ii} are statistically significant (*$p = 0.041$, $n = 3$)

opened at more negative membrane voltages, at which the driving force is greater, thus contributing to the higher current density observed in fed neurones. In addition, a more hyperpolarized activation curve is expected to lower the spike voltage threshold, thus increasing the excitability in hippocampal CA1 neurones of fed animals.

The presently reported differences in current density (and in voltage dependence of activation) could be due to hormonal cycles or gender-related physiological implications, rather than to a straightforward impact of fasting/feeding cycle. However, the same tendency, i.e. larger current densities, was also found in hippocampal CA1 neurones obtained from male rats (data not shown), which lead us to conclude that such variation is indeed attributed to fasting/feeding.

The feeding cycle also influenced the voltage dependence of inactivation of I_{Na}. The V_h parameter of h_∞ in fed neurones showed a significant depolarizing shift by 7 mV, in comparison to fasted neurones (see Table 1), reflecting an increase in the fraction of activatable channels.

By overlapping the activation and inactivation curves, we obtained a voltage range at which the activation occurs when the current is not completely inactivated—"window current" (French, Sah, Bucketr, Gage, & Curtin, 1990; Huang et al., 2011; Ketelaars et al., 2001). Again, the larger "window current" amplitude plus the negative shift observed in its voltage dependence emphasize the thesis of higher state of excitability in fed neurones.

The variation in the voltage dependence of h_∞ was accompanied by a depolarizing shift in the voltage dependence of τ_{hslow} observed in fed neurones, with slower values obtained at a hyperpolarized voltage range between −45 mV and −20 mV (see Figure 5b). In other words, I_{Na} displayed relatively less and slower inactivation in fed neurones in a wide range of potentials, which, once more, indicates a greater neuronal excitability after feeding. In addition, the ratio of the amplitude coefficients of fast and slow inactivating components of the time constant of inactivation (a_f/a_s) has been found to be increased in fed neurones (see Figure 5c). This is consistent with a greater variation in Na^+ channel expression at the surface of hippocampal CA1 neurones of fed animals. The dominance of the fast component over the slow component (ratio >1) suggests that such variation is most likely related to the differential expression of isoforms with faster kinetics, which is in accordance with the phenotype of Na^+ channel typically found in brain cells (Leterrier, Brachet, Fache, & Dargent, 2010; Vacher, Mohapatra, & Trimmer, 2008; Westenbroek, Merrick, & Catterall, 1989). Accordingly, LC-MS/MS analysis identified Nav1.2, a known fast inactivating isoform, as the major functional Na^+ channel alpha subunit of the rat hippocampus proteome.

Given the gathered evidence, we have assessed whether the feeding cycle determined variations in the expression levels of $Na_v1.2$ channel protein in hippocampal CA1 neurones. Despite the proteomic analysis presently reported has been

performed in the entire tissue of the rat hippocampus, one may assume that the results are representative of what happens on CA1 subfield neurones, where the electrophysiological experiments were carried out.

The western blotting experiments, run with whole-cell protein extracts and plasma membrane-enriched fractions of the rat hippocampus, pointed to a larger concentration of $Na_v1.2$ at the surface of hippocampal cells of fed animals. Hence, one may state that $Na_v1.2$ isoform underwent a differential surface expression whether animals have eaten or not. However, the greater Nav1.2 expression observed in plasma membrane-enriched fractions of fed samples contrasted with the constancy of Nav1.2 protein expression levels in whole-cell lysate extracts. Thus, despite the significantly increased number of functional Nav1.2 channels at the plasma membranes of fed samples, the cellular bulk production of Nav1.2 appears to be unaffected throughout the feeding cycle. Moreover, the rapid variation observed in the molecular availability of Na^+ channels during feeding cycle (1 hr feeding) might be explained by dissimilar Nav1.2 protein turnover rates at the neuronal plasma membrane or by a differentiated regulation of $Na_v1.2$ protein trafficking mechanisms to plasma membrane domains.

Ultimately, the cellular localization of $Na_v1.2$ channels in the central nervous system neurones—proximal Axon Initial Segment (AIS) – as well as their physiological function at ensuring action potential backpropagation, make them key players in the modulation of the threshold for the generation of somatodendritic potentials (Ahn, Beacham, Westenbroek, Scheuer, & Catterall, 2007; Hu et al., 2009; Westenbroek et al., 1989). Hence, in fed conditions, it is plausible to consider that a greater Nav1.2 channel density may result in a reduction in action potential threshold on hippocampal CA1 neurones, which, per se, promotes hyperexcitability.

We also assessed the effect of feeding cycle on the single channel Na^+ activity present at the soma of rat hippocampal CA1 neurones. Single-channel recordings were studied in the excised inside-out patch configuration. Unitary current amplitudes were measured by fitting all-points amplitude histograms with Gaussian curves. Fed neurones contained patches with higher current amplitude, suggesting an influence of feeding cycle over the unitary conductance. The calculated slope conductance for fed neurones was 16.7 pS, being consistent with the 16.6 pS value obtained in a previous study in rat hippocampal CA1 cells (Fernandes et al., 2001). The lower average single-channel conductance obtained for fasted neurones (12.6 pS) indicates an impact of feeding on the single-channel conductance: each Na^+ channel present at the surface of rat hippocampal CA1 neurones conducts more Na^+ ions through its pore during the post-prandial period, corroborating the results observed in the activation curves of whole-cell currents.

The single channel Na^+ current data also indicate that the impact of feeding cycle on Na^+ channel density might extent to other Na^+ channel isoforms (other than Nav1.2). For example, the Na^+ channel conductance of fed neurones is reminiscent of that obtained for SCN1A expressed in HEK-293 cells (17pS; Vanoye, Lossin, Rhodes, & George, 2006). This frames the Nav1.1 as a further molecular identity involved in the regulation of Na^+ channel expression by the feeding cycle. Hence, one can predict a larger $Na_v1.1$ channel number at the surface of the soma of hippocampal CA1 neurones of fed animals.

Our results clearly demonstrate that the feeding cycle modulates the functioning of Na^+ currents/channels of central pyramidal neurones, mainly confined to the CA1 region of rat hippocampus. Here, Nav1.2 expression levels and single channel Na^+ conductance may account for the modulation of whole cell Na^+ currents by the feeding cycle. Specifically, larger Nav1.2 channel density and higher single channel Na^+ conductance assigned to fed neurones are thought to be the foundations of the significant differences observed in the whole-cell current output. Furthermore, the differentiated Na^+ current response under fed vs. fasted conditions suggests an increase in intrinsic neuronal excitability upon feeding.

In summary, this study discloses a new perspective that brings together feeding cycle and rat hippocampal neurones. Feeding cycle induces a rapid and reversible adjustment of the biophysical and molecular characteristics of voltage-gated Na^+ currents of rat hippocampal CA1 pyramidal neurones. Such outcome elect the voltage gated Na^+ channels as potential molecular clues in the processing of satiety information by the hippocampus (Davidson et al., 2005, 2009; Hannapel et al., 2017; Hebben, Corkin, Eichenbaum, & Shedlack, 1985; Henderson, Nalloor, Vazdarjanova, & Parent, 2016; Henderson et al., 2013; Higgs, 2002; Hsu et al., 2015; Jacka et al., 2015; Kanoski & Grill, 2017; Parent et al., 2014; Parent, 2016b). Thus, when to eat, or how much to eat in any one meal are decisions that may rely on the functioning of Na^+ channels present at the surface of rat hippocampal neurones.

ACKNOWLEDGEMENTS

Financial support was provided by a PhD grant from Foundation for Science and Technology (FCT), Portugal (SFRH/BD/88199/2012), and by Sea4Us – Biotechnology and Marine Resources, Lda., Sagres, Portugal. The mass spectrometry experimental data were funded by a Prime XS project (PRIME-XS-000226).

CONFLICT OF INTERESTS

None of the authors has any conflict of interest to disclose. We confirm that we have read the Journal's position on issues

involved in ethical publication and affirm that this report is consistent with those guidelines.

DATA ACCESSIBILITY

Authors confirm that the data will be made available upon request.

AUTHOR'S CONTRIBUTIONS

AEPB performed all the experiments, being responsible for acquisition, analysis and interpretation of the data, and writing of the first draft of the manuscript. PFC helped in the interpretation of the data and revision of the manuscript for important intellectual content. SVM and MA were responsible for the acquisition, analysis and interpretation of the proteomics data. PAL contributed to the conception or design of the experiments, interpretation of the data, drafting of the outline, and revision of the manuscript for important intellectual content. All authors approved the final version of the manuscript and agree to be accountable for all aspects of the work.

ORCID

André E. P. Bastos https://orcid.org/0000-0002-0005-6640

REFERENCES

Afonso, R. A., Fernandes, A. B., Santos, C., Ligeiro, D., Ribeiro, R. T., Lima, I. S., … Macedo, M. P. (2012). Postprandial insulin resistance in Zucker diabetic fatty rats is associated with parasympathetic-nitric oxide axis deficiencies. *Journal of Neuroendocrinology*, *24*, 1346–1355. https://doi.org/10.1111/j.1365-2826.2012.02341.x

Ahn, M., Beacham, D., Westenbroek, R. E., Scheuer, T., & Catterall, W. A. (2007). Regulation of Na(v)1.2 channels by brain-derived neurotrophic factor, TrkB, and associated Fyn kinase. *Journal of Neuroscience*, *27*, 11533–11542. https://doi.org/10.1523/JNEUROSCI.5005-06.2007

Barry, P. H. (1994). JPCalc, a software package for calculating liquid junction potential corrections in patch-clamp, intracellular, epithelial and bilayer measurements and for correcting junction potential measurements. *Journal of Neuroscience Methods*, *51*, 107–116. https://doi.org/10.1016/0165-0270(94)90031-0

Beck, B., & Pourié, G. (2013). Ghrelin, neuropeptide Y, and other feeding-regulatory peptides active in the Hippocampus: Role in learning and memory. *Nutrition Reviews*, *71*, 541–561. https://doi.org/10.1111/nure.12045

Benoit, S. C., Davis, J. F., & Davidson, T. L. (2010). Learned and cognitive controls of food intake. *Brain Research*, *1350*, 71–76. https://doi.org/10.1016/j.brainres.2010.06.009

Bezanilla, F., & Armstrong, C. M. (1977). Inactivation of the sodium channel. I. Sodium current experiments. *The Journal of General Physiology*, *70*, 549–566. https://doi.org/10.1085/jgp.70.5.549

Boersema, P. J., Raijmakers, R., Lemeer, S., Mohammed, S., & Heck, A. J. R. (2009). Multiplex peptide stable isotope dimethyl labeling for quantitative proteomics. *Nature Protocols*, *4*, 484–494. https://doi.org/10.1038/nprot.2009.21

Bruehl, C., & Witte, O. W. (2003). Relation between bicarbonate concentration and voltage dependence of sodium currents in freshly isolated CA1 neurons of the rat. *Journal of Neurophysiology*, *89*, 2489–2498. https://doi.org/10.1152/jn.01083.2002

Cansev, M., van Wijk, N., Turkyilmaz, M., Orhan, F., Sijben, J. W. C., & Broersen, L. M. (2015). A specific multi-nutrient enriched diet enhances hippocampal cholinergic transmission in aged rats. *Neurobiology of Aging*, *36*, 344–351. https://doi.org/10.1016/j.neurobiolaging.2014.07.021

Costa, P. F. (1996). The kinetic parameters of sodium currents in maturing acutely isolated rat hippocampal CA1 neurones. *Brain Research. Developmental Brain Research*, *91*, 29–40. https://doi.org/10.1016/0165-3806(95)00159-X

Costa, P. F., Santos, A. I., & Ribeiro, M. A. (1994). Potassium currents in acutely isolated maturing rat hippocampal CA1 neurones. *Developmental Brain Research*, *83*, 216–223. https://doi.org/10.1016/0165-3806(94)00140-5

Cox, J., Matic, I., Hilger, M., Nagaraj, N., Selbach, M., Olsen, J. V., & Mann, M. (2009). A practical guide to the maxquant computational platform for silac-based quantitative proteomics. *Nature Protocols*, *4*, 698–705. https://doi.org/10.1038/nprot.2009.36

Davidson, T. L., Chan, K., Jarrard, L. E., Kanoski, S. E., Clegg, D. J., & Benoit, S. C. (2009). Contributions of the hippocampus and medial prefrontal cortex to energy and body weight regulation. *Hippocampus*, *19*, 235–252. https://doi.org/10.1002/hipo.20499

Davidson, T. L., & Jarrard, L. E. (1993). A role for hippocampus in the utilization of hunger signals. *Behavioral and Neural Biology*, *59*, 167–171. https://doi.org/10.1016/0163-1047(93)90925-8

Davidson, T. L., Kanoski, S. E., Schier, L. A., Clegg, D. J., & Benoit, S. C. (2007). A potential role for the hippocampus in energy intake and body weight regulation. *Current Opinion in Pharmacology*, *7*, 613–616. https://doi.org/10.1016/j.coph.2007.10.008

Davidson, T., Kanoski, S., Walls, E., & Jarrard, L. (2005). Memory inhibition and energy regulation. *Physiology & Behavior*, *86*, 731–746. https://doi.org/10.1016/j.physbeh.2005.09.004

Diano, S., Farr, S. A., Benoit, S. C., McNay, E. C., da Silva, I., Horvath, B., … Horvath, T. L. (2006). Ghrelin controls hippocampal spine synapse density and memory performance. *Nature Neuroscience*, *9*, 381–388. https://doi.org/10.1038/nn1656

Fernandes, J., Marvão, P., Santos, A. I., & Costa, P. F. (2001). Sodium channel currents in maturing acutely isolated rat hippocampal CA1 neurones. *Brain Research. Developmental Brain Research*, *132*, 159–174. https://doi.org/10.1016/S0165-3806(01)00312-1

French, C. R., Sah, P., Bucketr, K. J., Gage, P. W., & Curtin, J. (1990). A voltage-dependent persistent sodium current in mammalian hippocampal neurons. *Journal of General Physiology*, *95*, 1139–1157. https://doi.org/10.1085/jgp.95.6.1139

Gordon, D., Merrick, D., Auld, V., Dunn, R., Goldin, A. L., Davidson, N., & Catterall, W. A. (1987). Tissue-specific expression of the RI and RII sodium channel subtypes. *Proceedings of the National Academy of Sciences of the United States of America*, *84*, 8682–8686. https://doi.org/10.1073/pnas.84.23.8682

Hamill, O. P., Marty, A., Neher, E., Sakmann, B., & Sigworth, F. J. (1981). Improved patch-clamp techniques for high-resolution current recording from cells and cell-free membrane patches. *Pflügers*

Archiv – European Journal of Physiology, *391*, 85–100. https://doi.org/10.1007/BF00656997

Hannapel, R. C., Henderson, Y. H., Nalloor, R., Vazdarjanova, A., & Parent, M. B. (2017). Ventral hippocampal neurons inhibit postprandial energy intake. *Hippocampus*, *27*, 274–284. https://doi.org/10.1002/hipo.22692

Hebben, N., Corkin, S., Eichenbaum, H., & Shedlack, K. (1985). Diminished ability to interpret and report internal states after bilateral medial temporal resection: Case H.M. *Behavioral Neuroscience*, *99*, 1031–1039. https://doi.org/10.1037/0735-7044.99.6.1031

Henderson, Y. O., Nalloor, R., Vazdarjanova, A., & Parent, M. B. (2016). Sweet orosensation induces Arc expression in dorsal hippocampal CA1 neurons in an Experience-dependent manner. *Hippocampus*, *26*, 405–413. https://doi.org/10.1002/hipo.22532

Henderson, Y. O., Smith, G. P., & Parent, M. B. (2013). Hippocampal neurons inhibit meal onset. *Hippocampus*, *23*, 100–107. https://doi.org/10.1002/hipo.22062

Higgs, S. (2002). Memory for recent eating and its influence on subsequent food intake. *Appetite*, *39*, 159–166. https://doi.org/10.1006/appe.2002.0500

Hodgkin, A. L., & Huxley, A. F. (1952). The dual effect of membrane potential on sodium conductance in the giant axon of Loligo. *Journal of Physiology*, *116*, 497–506. https://doi.org/10.1113/jphysiol.1952.sp004719

Hsu, T. M., Hahn, J. D., Konanur, V. R., Noble, E. E., Suarez, A. N., Thai, J., … Kanoski, S. E. (2015). Hippocampus ghrelin signaling mediates appetite through lateral hypothalamic orexin pathways. *ELife*, *4*, 1–20.

Hsu, T. M., Suarez, A. N., & Kanoski, S. E. (2016). Ghrelin: A link between memory and ingestive behavior. *Physiology & Behavior*, *162*, 1–8.

Hu, W., Tian, C., Li, T., Yang, M., Hou, H., & Shu, Y. (2009). Distinct contributions of Nav1.6 and Nav1.2 in action potential initiation and backpropagation. *Nature Neuroscience*, *12*, 996–1002. https://doi.org/10.1038/nn.2359

Huang, H., Priori, S. G., Napolitano, C., O'Leary, M. E., & Chahine, M. (2011). Y1767C, a novel SCN5A mutation, induces a persistent Na+ current and potentiates ranolazine inhibition of Nav1.5 channels. *American Journal of Physiology-Heart and Circulatory Physiology*, *300*, H288–H299. https://doi.org/10.1152/ajpheart.00539.2010

Jacka, F. N., Cherbuin, N., Anstey, K. J., Sachdev, P., & Butterworth, P. (2015). Western diet is associated with a smaller hippocampus: A longitudinal investigation. *BMC Medicine*, *13*, 215. https://doi.org/10.1186/s12916-015-0461-x

Kanoski, S. E., & Davidson, T. L. (2011). Western diet consumption and cognitive impairment: Links to hippocampal dysfunction and obesity. *Physiology & Behavior*, *103*, 59–68. https://doi.org/10.1016/j.physbeh.2010.12.003

Kanoski, S. E., & Grill, H. J. (2017). Hippocampus contributions to food intake control: Mnemonic, neuroanatomical, and endocrine mechanisms. *Biological Psychiatry*, *81*, 748–756. https://doi.org/10.1016/j.biopsych.2015.09.011

Kay, A. R., & Wong, R. K. S. (1986). Isolation of neurons suitable for patch-clamping from adult mammalian central nervous systems. *Journal of Neuroscience Methods*, *16*, 227–238. https://doi.org/10.1016/0165-0270(86)90040-3

Ketelaars, S. O., Gorter, J., van Vliet, E., Lopes da Silva, F., & Wadman, W. (2001). Sodium currents in isolated rat CA1 pyramidal and dentate granule neurones in the post-status epilepticus model of epilepsy. *Neuroscience*, *105*, 109–120. https://doi.org/10.1016/S0306-4522(01)00176-2

Lathe, R. (2001). Hormones and the hippocampus. *Journal of Endocrinology*, *169*, 205–231. https://doi.org/10.1677/joe.0.1690205

Leterrier, C., Brachet, A., Fache, M. P., & Dargent, B. (2010). Voltage-gated sodium channel organization in neurons: Protein interactions and trafficking pathways. *Neuroscience Letters*, *486*, 92–100. https://doi.org/10.1016/j.neulet.2010.08.079

Lima, P. A., Costa, P. C., Mondragão, M., Alves, F. M., Costa, G., Hardy, D., … Auger., C. (2012) Metabolic states induced by feeding/fasting influence insulin-induced excitability and levels of insulin receptor in hippocampal but not cerebellar neurons. In *8 Th FENS Forum of Neuroscience* (p. 229). Barcelona, Spain: FENS, *e-book*.

Lima, P. A., Vicente, M. I., Alves, F. M., Dionísio, J. C., & Costa, P. F. (2008). Insulin increases excitability via a dose-dependent dual inhibition of voltage-activated K+ currents in differentiated N1E-115 neuroblastoma cells. *European Journal of Neuroscience*, *27*, 2019–2032. https://doi.org/10.1111/j.1460-9568.2008.06150.x

Ogden, D. (1994). *Microelectrode techniques: The Plymouth workshop handbook* (2nd ed.). Cambridge, UK: The Company of Biologists.

Palou, A., Remesar, X., Arola, L., Herrera, E., & Alemany, M. (1981). Metabolic effects of short term food deprivation in the rat. *Hormone and Metabolic Research*, *13*, 326–330. https://doi.org/10.1055/s-2007-1019258

Parent, M. B. (2016a). Dorsal hippocampal-dependent episodic memory inhibits eating. *Current Directions in Psychological Science*, *25*, 461–466. https://doi.org/10.1177/0963721416665103

Parent, M. B. (2016b). Cognitive control of meal onset and meal size: Role of dorsal hippocampal-dependent episodic memory. *Physiology & Behavior*, *162*, 112–119. https://doi.org/10.1016/j.physbeh.2016.03.036

Parent, M. B., Darling, J. N., & Henderson, Y. O. (2014). Remembering to eat: Hippocampal regulation of meal onset. *American Journal of Physiology: Regulatory, Integrative and Comparative Physiology*, *306*, R701–R713.

Ruben, P. C., Starkus, J. G., & Rayner, M. D. (1992). Steady-state availability of sodium channels. Interactions between activation and slow inactivation. *Biophysical Journal*, *61*, 941–955. https://doi.org/10.1016/S0006-3495(92)81901-X

Sah, P., Gibb, A. J., & Gage, P. W. (1988). The sodium current underlying action potentials in guinea pig hippocampal CAI neurons. *Journal of General Physiology*, *91*, 373–398. https://doi.org/10.1085/jgp.91.3.373

Sakmann, B., & Neher, E. (1995). *Single-channel recording* (2nd ed.). New York, NY: Plenum Press.

Scoville, W. B., & Milner, B. (1957). Loss of recent memory after bilateral hippocampal lesions. *Journal of Neurology, Neurosurgery and Psychiatry*, *20*, 11–21. https://doi.org/10.1136/jnnp.20.1.11

Stangl, D., & Thuret, S. (2009). Impact of diet on adult hippocampal neurogenesis. *Genes & Nutrition*, *4*, 271–282. https://doi.org/10.1007/s12263-009-0134-5

Sun, G. Y., Huang, H. M., Kelleher, J. A., Stubbs, E. B., & Sun, A. Y. (1988). Marker enzymes, phospholipids and acyl group composition of a somal plasma membrane fraction isolated from rat cerebral cortex: A comparison with microsomes and synaptic plasma membranes. *Neurochemistry International*, *12*, 69–77. https://doi.org/10.1016/0197-0186(88)90150-7

Sweeney, P., & Yang, Y. (2015). An excitatory ventral hippocampus to lateral septum circuit that suppresses feeding. *Nature Communications*, *6*, 10188. https://doi.org/10.1038/ncomms10188

Sweeney, P., & Yang, Y. (2017). Neural circuit mechanisms underlying emotional regulation of homeostatic feeding. *Trends in Endocrinology and Metabolism*, *28*, 437–448. https://doi.org/10.1016/j.tem.2017.02.006

Tracy, A. L., Jarrard, L. E., & Davidson, T. L. (2001). The hippocampus and motivation revisited: Appetite and activity. *Behavioral Brain Research*, *127*, 13–23. https://doi.org/10.1016/S0166-4328(01)00364-3

Vacher, H., Mohapatra, D. P., & Trimmer, J. S. (2008). Localization and targeting of voltage-dependent ion channels in mammalian central neurons. *Physiological Reviews*, *88*, 1407–1447. https://doi.org/10.1152/physrev.00002.2008

Vanoye, C. G., Lossin, C., Rhodes, T. H., & George, A. L. (2006). Single-channel properties of human Na V 1.1 and mechanism of channel dysfunction in SCN1A -associated epilepsy. *The Journal of General Physiology*, *127*, 1–14. https://doi.org/10.1085/jgp.200509373

Vedantham, V., & Cannon, S. C. (1998). Slow inactivation does not affect movement of the fast inactivation gate in voltage-gated Na+ channels. *Journal of General Physiology*, *111*, 83–93. https://doi.org/10.1085/jgp.111.1.83

Vreugdenhil, M., Faas, G. C., & Wadman, W. J. (1998). Sodium currents in isolated rat CA1 neurons after kindling epileptogenesis. *Neuroscience*, *86*, 99–107. https://doi.org/10.1016/S0306-4522(98)00041-4

Westenbroek, R. E., Merrick, D. K., & Catterall, W. A. (1989). Differential subcellular localization of the RI and RII Na+ channel subtypes in central neurons. *Neuron*, *3*, 695–704. https://doi.org/10.1016/0896-6273(89)90238-9

Wiśniewski, J. R., Zougman, A., Nagaraj, N., & Mann, M. (2009). Universal sample preparation method for proteome analysis. *Nature Methods*, *6*, 359–362. https://doi.org/10.1038/nmeth.1322

Yeomans, M. R. (2017). Adverse effects of consuming high fat–sugar diets on cognition: Implications for understanding obesity. *Proceedings of the Nutrition Society*, *76*, 455–465. https://doi.org/10.1017/S0029665117000805

How to cite this article: Bastos AEP, Costa PF, Varderidou-Minasian S, Altelaar M, Lima PA. Feeding cycle alters the biophysics and molecular expression of voltage-gated Na^+ currents in rat hippocampal CA1 neurones. *Eur J Neurosci*. 2019;49:1418–1435. https://doi.org/10.1111/ejn.14331